Analysis of the structural changes of a pellet/powder bentonite mixture upon wetting by X-ray computed microtomography

Agustín Molinero Guerra, Patrick Aimedieu, Michel Bornert, Yu-Jun Cui, Anh Minh A.M. Tang, Zhao Sun, Nadia Mokni, Pierre Delage, Frédéric Bernier

To cite this version:

Analysis of the structural changes of a pellet/powder bentonite mixture upon wetting by X-ray computed microtomography

Agustín Molinero Guerra[1,2], Patrick Aimedieu[1], Michel Bornert[1], Yu-Jun Cui[1], Anh Minh Tang[1*], Zhao Sun[3], Nadia Mokni[2], Pierre Delage[1], Frédéric Bernier[4]

[1]Ecole des Ponts ParisTech, CNRS, IFSTTAR, Laboratoire Navier/CERMES, Marne La Vallée, France
[2]Institut de Radioprotection et de Sûreté Nucléaire (IRSN), Fontenay-aux-Roses, France
[3]Tongji University, China
[4]Agence Fédérale de Contrôle Nucléaire (AFCN), Belgium

*Corresponding author

Dr. Anh Minh Tang

Ecole des Ponts ParisTech
6-8 av. Blaise Pascal
Cité Descartes, Champs-sur-Marne
77455 Marne la Vallée
France

E-mail: anhminh.tang@enpc.fr

Abstract:

Pellet/powder bentonite mixture is one of the candidate materials for sealing plugs in deep geological high-level radioactive waste disposal. This note presents an investigation on the structure changes of this mixture occurring during the saturation process by means of X-ray computed micro-tomography. The test was performed in an infiltration column (60 mm in inner diameter and 120 mm in height). Water was supplied to the two ends of the column and the changes of the sample morphology were observed during a period of 100 days of hydration. Digital Volume Correlation (DVC) technique was used to determine the vertical displacement field of the bentonite powder. A pressure transducer was used to measure the axial swelling pressure during the hydration. The results show that the initial distribution of powder in the inter-pellet pores was not homogeneous; the powder filled almost completely the pores in the zones close to the two ends while air-filled inter-pellet voids were observed in the middle of the column specimen. When water started to infiltrate inside the specimen from both ends, the pellets and the powder grains started to swell (because of the swelling properties of smectite, the principal mineral of bentonite) and filled the voids. That induced at the same time increase of swelling pressure and downward movement of powder grains. The results allowed a better understanding on the hydro-mechanical couplings, at the pellet scale, in the pellet/powder bentonite mixture upon wetting.

Keywords: pellet/powder bentonite mixture; X-ray computed microtomography; initial heterogeneity; Digital Volume Correlation; water saturation; homogenization.

1. Introduction

In the context of deep geological high-level radioactive waste disposal, non-compacted pellet/powder bentonite mixtures are considered as candidate sealing materials because of their high swelling capacity and high radionuclide migration retardation properties, as well as their operational advantages: they are easy to transport, install, and allow gaps between the rock and the seal to be minimized. In a real repository this unsaturated mixture will be installed to plug galleries. Then, water coming from the host rock will start saturating the mixture under almost constant-volume conditions. The swollen mixture will fill different voids and generate swelling pressure, ensuring the sealing of the storage system. Molinero Guerra et al. (2017) used X-ray computed tomography (X-ray CT) to investigate the microstructure of pellet/powder bentonite and found that this mixture was characterized by an initial heterogeneous distribution of powder grains inside the inter-pellet pores. This initial state could greatly influence the saturation process and the corresponding structure changes. As a result, the overall hydro-mechanical behavior would change during the saturation process. Therefore, to properly assess the safety of the underground radioactive waste disposal, it is of paramount importance to well understand the microstructure change of the mixture in the course of hydration.

In this context, the Institute of Radioprotection and Nuclear Safety (IRSN, France), as a part of the overall research and development program that aims at providing scientific background for disposal safety, launched the SEALEX (SEALing performance EXperiments) project, within which this work was conducted. It consists of a series of full-scale experiments carried out in IRSN's Underground Research Laboratory (URL – Tournemire, France) (Barnichon & Deleruyelle, 2009; Mokni & Barnichon, 2016) and small-scale experiments conducted in the laboratory (Wang et al., 2012; Saba et al., 2014). One of the aims of the full-scale experiments was to test the long-term hydraulic performance of sealing systems in normal conditions for

78   different clay core compositions (pure bentonite or bentonite/sand mixtures) and

79   conditionings (pre-compacted blocks, mixture of pellets/powder, or in-situ compacted). In the

80   present work, a pellet/powder bentonite mixture with a proportion of 80/20 in dry mass was

81   investigated.

82   The hydro-mechanical behavior of engineered barriers composed of compacted

83   bentonite/sand mixtures or compacted pure bentonite has been extensively investigated (e.g.

84   Pusch 1982; Graham et al., 1989; Komine & Ogata, 1994; Dixon et al., 1996; Alonso et al.,

85   2005; Wang et al., 2013b, 2014; Saba et al., 2014; Sun et al., 2014). However, few studies

86   have been carried out on the mixture of pellet and powder of bentonite. Imbert & Villar

87   (2006) performed infiltration tests on a pellet/powder bentonite mixture and found that the

88   swelling pressure was analogous to that of a specimen of compacted powder at the same dry

89   density. Garcia-Siñeriz et al. (2015) studied the homogenization process of a material made of

90   bentonite pellets through a large-scale experiment on engineered barrier (EB). Upon

91   dismantling after 12 years of operation, a gradient of density and water content was still found

92   within the mixture because of the initial heterogeneity of the material. Van Geet et al. (2005)

93   investigated the hydration process of a pellet/powder bentonite mixture by X-ray CT. A

94   progressive decrease of the pellets density and an apparent homogenous sample after

95   saturation were observed. However, in the work of Van Geet et al. (2005), a cylindrical cell

96   containing only few pellets was used. As a result, the analyses mainly focused on the scale of

97   a single pellet.

98   The present work was thus conducted to investigate the structural changes of a pellet/powder

99   bentonite mixture with a large number of pellets by X-ray CT. Firstly, the sealing capacity of

100 the mixture and its structural evolution during saturation were studied. Secondly, Digital

101 Volume Correlation (DVC) technique was applied to calculate the displacement field within

102 the sample. Finally, the evolution of the axial swelling pressure while wetting was

4

103   investigated. The obtained results provide helpful elements to assess the hydromechanical

104   performance of seals/plugs made up of this kind of bentonite mixtures.

105   ## 2. Material and methodology

106   ## 2.1. Pellet/powder MX80 bentonite mixture

107   The soil studied was a mixture of pellet/powder MX80 bentonite (from Wyoming, USA) at a

108   proportion of 80/20 in dry mass. It was provided by the Laviosa-MPC Company under the

109   commercial name Expangel SP7 for pellets and SP30 for the powder, both were produced

110   from the same bentonite. The bentonite had a smectite content of 80%, other minerals being

111   quartz, calcite and pyrite. The CEC was 98 meq/100 g and the major exchangeable cations

112   were: sodium (52 cmol(+)/kg), calcium (37 cmol(+)/kg), magnesium (10 cmol(+)/kg). The

113   liquid limit was 560%, the plastic limit was 62% and the unit mass of the solid particles was

114   2.77 Mg/m^3 (Saba et al. 2014).

115   Cylindro-spherical pellets of bentonite were produced by compacting commercial bentonite

116   powder in a mold of 7 mm in diameter and 7 mm in height. The initial suction ($s = 135 \pm 3$

117   MPa) was measured in the laboratory with a chilled mirror dew point tensiometer (Decagon

118   WP4C), corresponding to an initial water content w = 5% - 7%. The initial void ratio of the

119   pellets was $e = 0.306 - 0.386$ (corresponding to a dry density of $2.00 - 2.12$ Mg/m^3) and the

120   degree of saturation was $S_r = 55\% - 66\%$. The bentonite powder was produced by crushing

121   pellets. An initial water content of 3% (smaller than that of the pellets) was found in the

122   laboratory, corresponding to an initial suction s = 191 MPa (equally measured by a chilled

123   mirror dew point tensiometer).

124   The saturation fluid was obtained by mixing the chemical components presented in Table 1

125   with distilled water until full dissolution. The resulting synthetic water had the same chemical

126   composition as the pore water of the Callovo-Oxfordian claystone (a possible geological host

5

127 rock for radioactive waste disposal in France) from the underground research laboratory in

128 Bure (Wang et al., 2013*a*). The table shows a total mass of 5.677 g of salt per liter of solution,

129 that corresponded to a salinity (mass of salt per mass of solution) lower than 1%.

2.2. Experimental set-up

131 A special set-up was designed to carry out X-ray CT observations on the pellet/powder

132 mixture while wetting. The layout is presented in Figure 1a. It consists of a transparent

133 PMMA (PolyMethyl MethAcrylate) cell of 60 mm in inner diameter and 120 mm in height

134 (corresponding to 1/10 scale of the SEALEX full-scale experiment). In the full-scale

135 experiment, a horizontal borehole, with a 0.60-m diameter and 5.40-m length was excavated

136 in the Tournemire URL, located in a Mesozoic sedimentary basin on the western edge of the

137 French Causses. The clay-based core, which represented the engineered clay barrier, had a

138 total length of 1.20 m. The laboratory specimen was installed between two porous stones and

139 filter papers, placed at its top and bottom. The constant-volume condition for the

140 pellet/powder bentonite mixture was ensured by the rigid PMMA cell and a top piston which

141 could prevent axial swelling. The mixture was saturated from both sides (top and bottom),

142 simulating the SEALEX in situ experiments (in the full-scale experiment, the clay-based core

143 was saturated with water from both ends with a small pressure of 10 kPa). The axial swelling

144 pressure was monitored during the test with a force transducer. The base and top were both

145 equipped with a water inlet and an air outlet. Figure 1b shows the PMMA cell positioned

146 inside the X-ray microtomograph. The cell was connected to two reservoirs (located at the top

147 and bottom of the sample) allowing water infiltration. The visualized parameter from X-ray

148 CT observations was the linear attenuation coefficient, which was represented as a grey level.

149 This parameter depended on density, the atomic number and the used X-ray energy.

2.3. Sample preparation and test protocol

151 The pellet/powder mixture was prepared by following the first protocol proposed in Molinero

152 Guerra et al. (2017) to obtain a homogeneous pellet/powder distribution within the sample at

153 the target dry density (1.49 Mg/m^3). It consists in filling the cell by packets corresponding to

154 one layer of pellets spread over its base and by adding the corresponding amount of powder

155 (considering the proportion 80-pellet/20-powder in dry mass). The density of the mixture was

156 checked with the mass of the bentonite (with known water content) used to fill the cell (with

157 known volume). Moreover, some reference elements of 1500 PMMA spheres of 1.6 mm

158 diameter (density 1.18-1.19 Mg/m^3) were randomly distributed within the sample during the

159 preparation process. The purpose was to carry out quantitative analyses of bentonite powder

160 displacement by DVC technique. DVC is a full-field measurement technique that basically

161 consists in comparing two pictures at two different stages and calculating a displacement

162 field. A detailed description of this technique can be found in Sutton et al. (2009) and Bornert

163 et al. (2012).

164 The general experiment scheme consisted in scanning the pellet/powder mixture at different

165 times during the saturation process. This resulted in a kind of incremental scans occurring

166 during the hydration process: several X-ray CT observations were carried out at different

167 times until an apparent homogeneous mixture was observed. Each scan took 19 h. Prior to

168 each X-ray CT scan, the whole system shown in Figure 1a was moved and installed inside the

169 microtomograph.

170 The first step of the test consisted in opening the water inlet valves. Air inside the system was

171 evacuated by opening the air outlet valve until no air bubble could be observed anymore in

172 the outlets. Water was supplied through both the top and bottom of the sample, as in the

173 SEALEX full-scale experiments, during the total time of the test with no pressure. Axial

174 swelling pressure was recorded automatically by a force transducer and a numerical data

175 logger.

3. Results

3.1. Qualitative analyses

The behavior of the pellet/powder mixture was firstly investigated by carrying out a qualitative analysis of the X-ray CT observations. Figure 2 shows a vertical section obtained at different times.

Initially, the mixture had a heterogeneous distribution of pellets and powder in spite of a careful preparation procedure. Air-filled inter-pellet voids were dominant in the zone between the bottom and 90-mm height. Above this zone, bentonite powder was more dominant in the inter-pellet voids. The top of the mixture was characterized by the presence of larger air-filled voids between the mixture and the porous stone, most probably due to segregation in the fabrication process. In-depth characterization of a mixture composed of pellet/powder bentonite can be found in Molinero Guerra et al. (2017).

After 2 days of hydration, the voids on the top of the specimen were completely sealed due to their vicinity to the hydration front, so the material at this level swelled quickly. The swelling properties of the material corresponded to the swelling properties of smectite, which was the principal mineral of bentonite. It can be deduced from sections corresponding to 2 days and 4 days after hydration that the evolution of the top hydration front was quicker than the bottom one. Afterwards the evolution of both hydration fronts was similar. The initial structure lost its granular nature while wetting; air-filled inter-pellet voids were still visible after 56 days of hydration, even though the pellets located at the furthest position from both hydration fronts had already swollen at this time. An apparently global homogeneous sample was observed after 100 days of hydration. At this time, almost all the air-filled inter-pellet voids had been completely sealed. In this figure, a glass sphere with a diameter of 10 mm can be seen; this

199   element was introduced to the specimen during its preparation as a reference material for X-

200   ray CT analysis.

201   To better understand the transition between the initial state and the final one, an enlargement

202   of a horizontal section at 60 mm from the bottom hydration front is presented in Figure 3.

203   Initially, high-density pellets could be observed with several powder grains between them.

204   After 11 days of hydration, some cracks developed within the pellets due to the decrease of

205   suction. As was observed by Molinero Guerra et al. (2017), cracks were already part of the

206   initial state of the pellet; they appeared during the storage in the laboratory combined to the

207   fabrication process of a single pellet. Those cracks could not be observed in this work, due to

208   the insufficient resolution of the X-ray CT observations (50 μm/voxel) as compared to the

209   resolution that was used to study a single pellet (4.4 μm/voxel); however, it is most probable

210   that they were already present at the initial state and opened while wetting. Wetting induced

211   swelling of smectite particles, enhanced these cracks and made them visible after 11 days of

212   hydration. After 27 days, more cracks were observed, as well as the decrease of the inter-

213   pellet voids due to swelling. Then, pellets started losing their granular structure. After 56

214   days, pellets could still be identified even if they had almost lost their initial granular

215   structure; some air-filled inter-pellet voids were observed. Therefore, the evolution of the

216   structure of a single pellet was characterized by the development of cracks combined to the

217   swelling of its components.

218   Van Geet et al. (2005) investigated the homogenization process of a pellet/powder mixture by

219   performing an analysis of the X-ray CT results. They noticed the decrease of the pellet density

220   while wetting and the final homogenization at complete saturation. In the present work, a

221   vertical section was investigated in order to ensure the total homogenization at the studied

222   resolution along the specimen's height, as well as the sealing of all air-filled voids within the

223   mixture.

3.2. Quantitative analyses

3.2.1. Evolution of the axial swelling pressure

The evolution of the axial swelling pressure during wetting was monitored during the test thanks to a force transducer installed at the bottom of the sample (see Figure 1). Results are presented in Figure 4 for the 160 days of hydration. Due to the design of the cell, this value corresponded to the average force transmitted to the porous stone at the bottom of the sample. A plateau of 3 MPa was reached after 100 days of hydration. In the work of Molinero-Guerra et al. (2018), an infiltration column test was performed on the same material with the same conditions. The results showed the same kinetics of the axial swelling pressure (it increased and reached a plateau after 100 days, but at 2.5 MPa).

After Wang et al. (2012, 2013c), the swelling pressure of pure bentonite, mixture of bentonite/sand, and mixture of bentonite/claystone can be correlated with the dry density of bentonite at the final (fully-saturated) state. A unique equation was proposed to predict the swelling pressure of MX80 bentonite-based materials from the dry density of bentonite. In addition, these works evidenced that the swelling pressure obtained by using synthetic Callovo-Oxfordian claystone water was similar to that obtained by using distilled water due to the low salinity of this synthetic water. Based on the equation proposed by Wang et al. (2012), for a dry density of the mixture of 1.49 Mg/m^3 the axial swelling pressure value should equal to 4.15 MPa. This value is higher than those observed in infiltration columns in the present work and in the work of Molinero-Guerra et al. (2018). It is possible that the sample was not completely saturated and the plateau observed did not correspond to the final swelling pressure value.

3.2.2. Investigation of the displacement field of the bentonite powder

247   DVC technique was used to calculate the displacement field of PMMA spheres added to the

248   sample during the fabrication process. Figure 5 presents the results, which correspond to

249   vertical displacements occurring during the first 100 days of hydration (positive value

250   corresponds to an upward displacement; μ and σ represent average and standard deviation

251   values of the displacement, respectively). For each location (height), the displacements of

252   spheres located at ±10 mm in the vertical direction were considered, and finally the mean

253   value was calculated.

254   The results show a sudden displacement of $0.2 - 0.4$ mm of the PMMA spheres towards the

255   bottom after 2 days of hydration for the locations at 30, 50, 70 and 110 mm. Actually, these

256   locations correspond to the zone where air-filled inter-pellet voids were dominant (Figure 2).

257   Hydration induced swelling of the material at both ends, increasing the swelling pressure

258   (Figure 4), and provoked pellets re-arrangement. The movement of pellets would then induce

259   the movement of bentonite powder and PMMA spheres located in the inter-pellet voids. As

260   air-filled inter-pellet voids were dominant in these zones, bentonite powder and PMMA

261   spheres would tend to move downward because of gravity. This phenomenon was less visible

262   at 10 mm from the bottom because the bottom partly restricted this movement. At 90 mm, a

263   heave was observed during the first 2 days of hydration. First, the downward displacement of

264   PMMA spheres should have been limited in this zone because bentonite powder was

265   relatively dominant in the inter-pellet voids (see Figure 2). Second, material in this zone

266   would have tended to heave to fill the initial gap at the top during these first two days.

267   The above phenomena continued generally with the same trends until 11 days of hydration.

268   After this date, the movement of the PMMA sphere was negligible until 49 days of hydration.

269   Between 49 days and 56 days of hydration, a sudden downwards movement was found at all

270   the levels (except at 10 mm from the bottom). This movement might be explained by the

271   movement of the cell during its installation; the cell (the whole system shown in Figure 1a)

11

272   was removed from the microtomograph and put back to its position only during the duration

273   of the scans. This phenomenon might be equally used to explain the general downward

274   displacement between 56 days and 100 days of hydration.

275   4. Conclusions

276   The wetting-induced structure changes of a pellet/powder bentonite mixture, one of the

277   candidate materials for sealing plugs in deep geological high-level radioactive waste disposal,

278   were investigated in this work by X-ray CT observations.

279   The results show that the initial mixture was a heterogeneous granular material since the

280   distribution of pellets and powder was not spatially uniform. While wetting the top and

281   bottom sides, water infiltrated quickly into the inter-pellet pores in the vicinity of both

282   hydration fronts. That induced rapid swelling of pellets and powder of bentonite due to the

283   absorption of water by smectite, the principal mineral of bentonite. Firstly, X-ray CT

284   observations showed that the initial granular structure was quickly lost in these zones; pellets

285   lost their structure and the mixture became an apparently homogeneous material, with no

286   more air-filled inter-pellet voids. For the rest of the sample, this process depended on the

287   evolution of the hydration front. Secondly, at the same time, swelling of pellets induced their

288   re-arrangement which caused downward movement of the bentonite powder, induced by

289   gravity, in the zones having large air-filled inter-pellet voids. This phenomenon enhanced the

290   heterogeneous spatial distribution of bentonite powder inside the mixture. Finally, swelling of

291   pellets and the powder grains induced a quick increase of axial swelling pressure that reached

292   3 MPa after 100 days. This value was lower that the estimated swelling pressure of the same

293   material having identical average dry density after full saturation. This result suggested that

294   the mixture was not fully saturated after 100 days of hydration even if the X-ray CT

295   observations showed a relatively homogeneous structure at this time.

296 The results in this study allowed visualizing water infiltration inside the pellet/powder

297 bentonite mixture during hydration. That would contribute to a better understanding on the

298 hydro-mechanical couplings in this material, when it is installed in the real repository.

References

300 Alonso, E.E., Romero, E., Hoffmann, C., & Garcia-Escudero, E., (2005). Expansive
301 bentonite-sand mixtures in cyclic controlled-suction drying and wetting. *Engineering*
302 *Geology*, 81(3), pp.213–226.

303 Bornert, M., Hild, F., Orteu, J.-J. and Roux, S. (2012). Chapter 6: digital image correlation.
304 In: Full-field measurements and identification in solid mechanics. Grediac, M. & Hild, F.
305 (Eds), Wiley-ISTE, 496 pages

306 Dixon D. A. Gray M. N. & Graham J., (1996). Swelling and hydraulic properties of
307 bentonites from Japan, Canada and the USA. Environmental Geotechnics 1, 43-48.

308 Barnichon, J.D., Deleruyelle, F., (2009). Sealing Experiments at the Tournemire URL.
309 EUROSAFE.

310 Garcia-Siñeriz, J. L., Villar, M. V., Rey, M., and Palacios, B., 2015. "Engineered barrier of
311 bentonite pellets and compacted blocks: State after reaching saturation," Eng. Geol., vol.
312 192, pp. 33–45.

313 Graham, J., Saadat, F., Gray, M. N., Dixon, D. A., & Zhang, Q. Y., (1989). Strength and
314 volume change behaviour of a sand-bentonite mixture. Canadian Geotechnical Journal
315 26, No. 2, 292- 305.

316 Herman, G.T. (1979). Correction for beam hardening in computed tomography. Physicsin
317 Medicine andBiology, 24, 81.

318 Imbert, C. & Villar, M.V., (2006). Hydro-mechanical response of a bentonite pellets/powder
319 mixture upon infiltration. *Applied Clay Science*, 32(3-4), pp.197–209.

320 Komine, H., & Ogata, N., (1994). Experimental study on swelling characteristics of
321 compacted bentonite. Canadian geotechnical journal 31 , No. 4, 478-490.

322 Molinero-Guerra, A., Mokni, N., Delage, P., Cui, Y. J., Tang, A. M., Aimedieu, P., Bernier,
323 F., Bornert, M., (2017). In-depth characterisation of a mixture composed of
324 powder/pellets MX80 bentonite. Applied Clay Science (135), 538 – 546.

325 Molinero-Guerra, A., Cui, Y.J., Mokni, N., Delage, P., Bornert, M., Aimedieu, P., Tang,
326 A.M., & Bernier, F., (2018). Investigation of the hydro-mechanical behaviour of a
327 pellet/powder MX80 bentonite mixture using an infiltration column. Engineering
328 Geology, 243, 18 – 25.

329 Mokni, N. & Barnichon, J.D., (2016). Hydro-mechanical analysis of SEALEX in situ tests-
330   Impact of technological gaps on long term performance of repository seals. Engineering
331   Geology, 205, pp. 81-92.

332 Pusch, R. (1982). Mineral-water interactions and their influence on the physical behavior of
333   highly compacted Na bentonite. Canadian Geotechnical Journal, 19(3): 381–387.
334   doi:10.1139/t82-041.

335 Saba, S., Cui, Y.J. and Barnichon, J.D., (2014). Investigation of the swelling behaviour of
336   compacted bentonite–sand mixture by mock-up tests. Canadian Geotechnical Journal,
337   51(12), pp.1399–1412.

338 Sun, W., Sun, D., Fang, L. & Liu, S., (2014). Soil-water characteristics of Gaomiaozi
339   bentonite by vapour equilibrium technique. *Journal of Rock Mechanics and
340   Geotechnical Engineering*, 6(1), pp.48–54.

341 Sutton, M.A., Orteu, J.J., and H. Schreier., H., (2009). Image correlation for shape, motion
342   and deformation measurements: basic concepts, theory and applications. Springer
343   Science & Business Media.

344 Van Geet, M., Volckaert, G. & Roels, S., (2005). The use of microfocus X-ray computed
345   tomography in characterising the hydration of a clay pellet/powder mixture. *Applied
346   Clay Science*, 29(2), pp.73–87.

347 Wang, Q., Tang, A.M., Cui, Y.J., Delage, P., Gatmiri, B., (2012). Experimental study on the
348   swelling behaviour of bentonite/claystone mixture. Eng. Geol. 124, 59–66. http://dx.
349   doi.org/10.1016/j.engeo.2011.10.003.

350 Wang, Q. & Cui, Y.J., Tang, A.M., Delage, P., Gatmiri, B. and Ye, WM., (2013a). Long-term
351   effect of water chemistry on the swelling pressure of a bentonite-based material. *Applied
352   Clay Science*. 87. 10.1016/j.clay.2013.10.025.

353 Wang, Q., Cui, Y. J., Tang, A. M., Barnichon, J. D., Saba, S. & Ye, W. M., (2013b).
354   Hydraulic conductivity and microstructure changes of compacted bentonite/sand mixture
355   during hydration. *Engineering Geology*, 164, pp.67–76.

356 Wang, Q., Tang, A.M., Cui, Y.J., Delage, P., Barnichon, J.D., Ye, W.M. (2013c). The effects
357   of technological voids on the hydro-mechanical behaviour of compacted bentonite-sand
358   mixture. *Soils and Foundations*, 53(2), 232 – 245.

359 Wang, Q., Cui, Y. J., Tang, A. M., Li, X. L. & Ye, W. M., (2014). Time- and density-
360   dependent microstructure features of compacted bentonite. *Soils and Foundations*, 54(4),
361   pp.657–666.

362

363

List of Tables

Table 1. Chemical composition of the synthetic water.

List of Figures

378 **Tables**

379 Table 1. Chemical composition of the synthetic water.

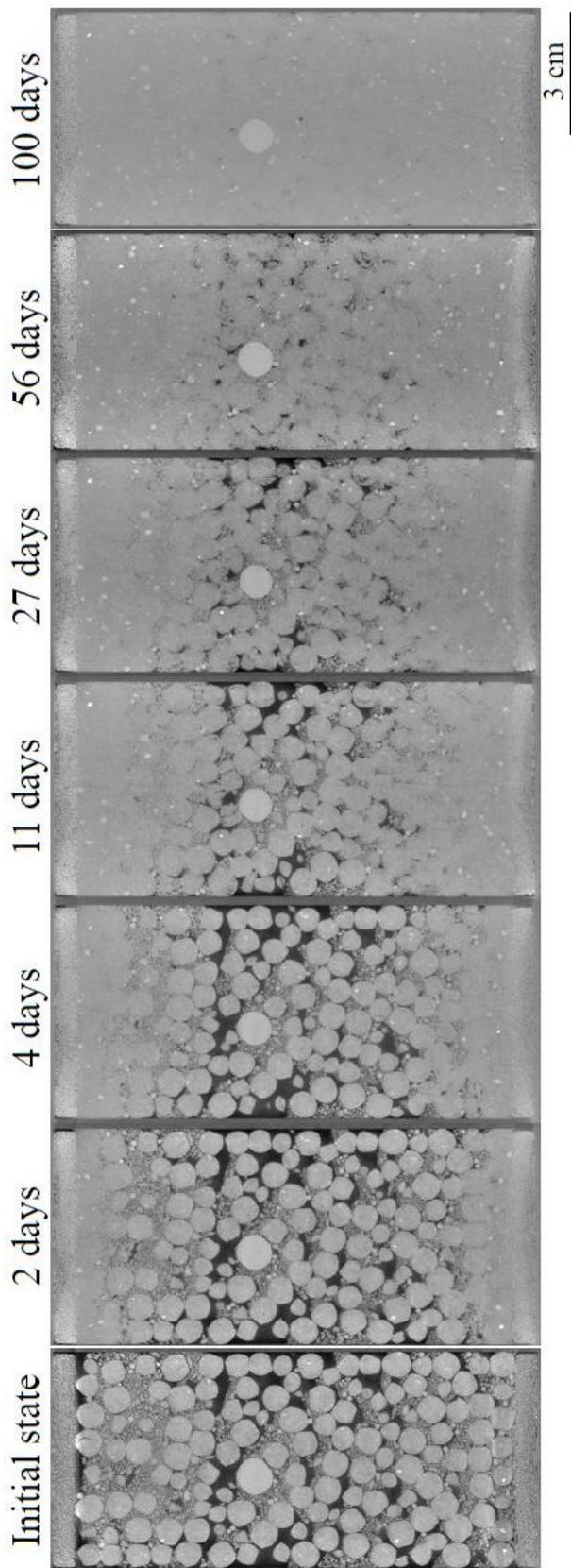| Components	NaHCO$_3$	Na$_2$SO$_4$	NaCl	KCl	CaCl$_2$ 2H$_2$O	MgCl$_2$O6H$_2$O	SrCl$_2$6H$_2$O	Total
Mass (g) per liter of solution	0.28	2.216	0.615	0.075	1.082	1.356	0.053	5.677

380

381

Figures

Figure 1. Photography of the experimental set-up inside the X-ray microtomograph device (b) and layout of the cell (a).
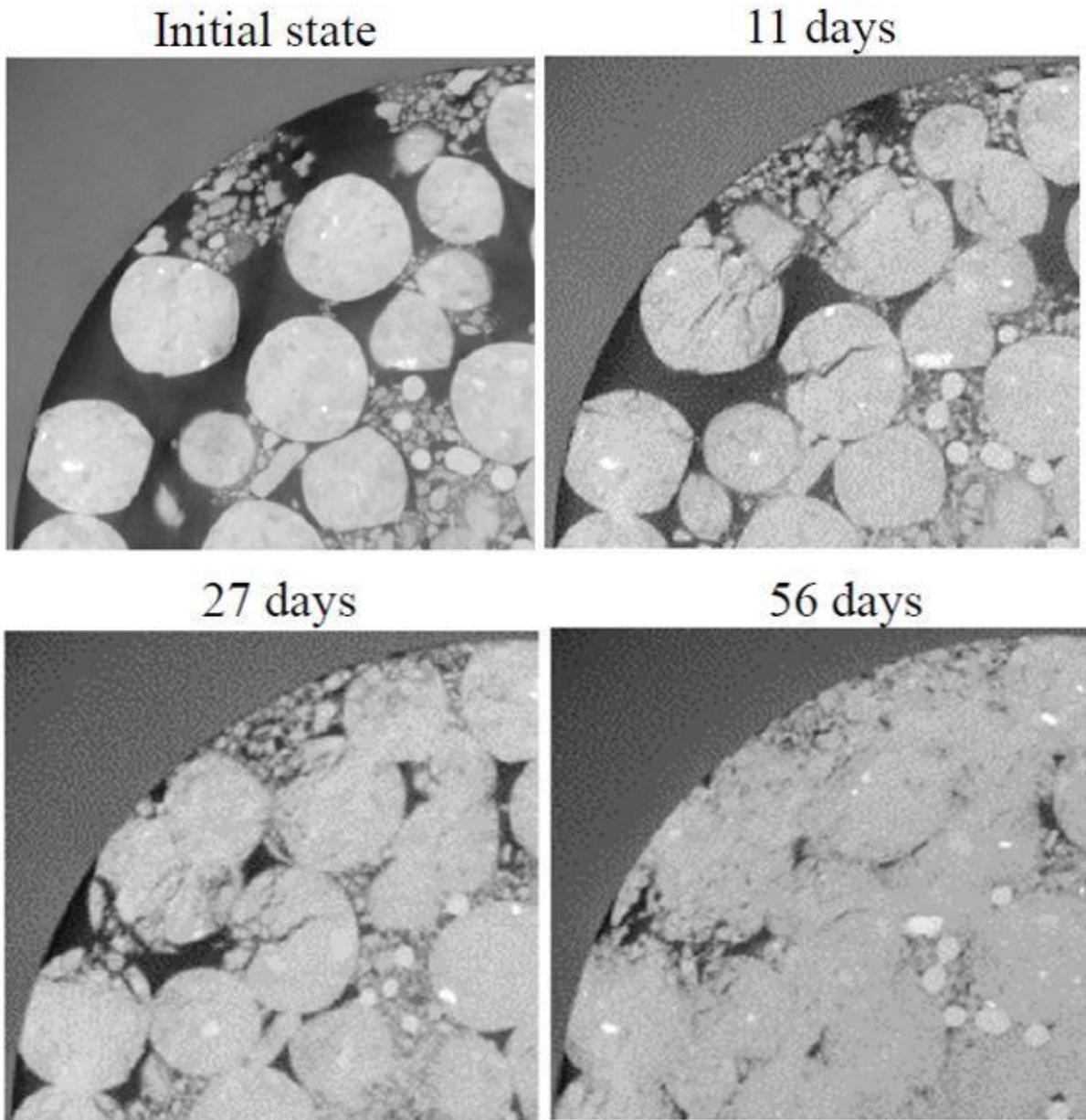

(a)

Water tank

Air outlet   Water inlet

Porous stone

PMMA cell   30   60   120

Porous stone

Air outlet   Water inlet
Force transudcer

(b)

1. Water tank – bottom
2. Water tank – top
3. Sample
4. Filter
5. Force transducer
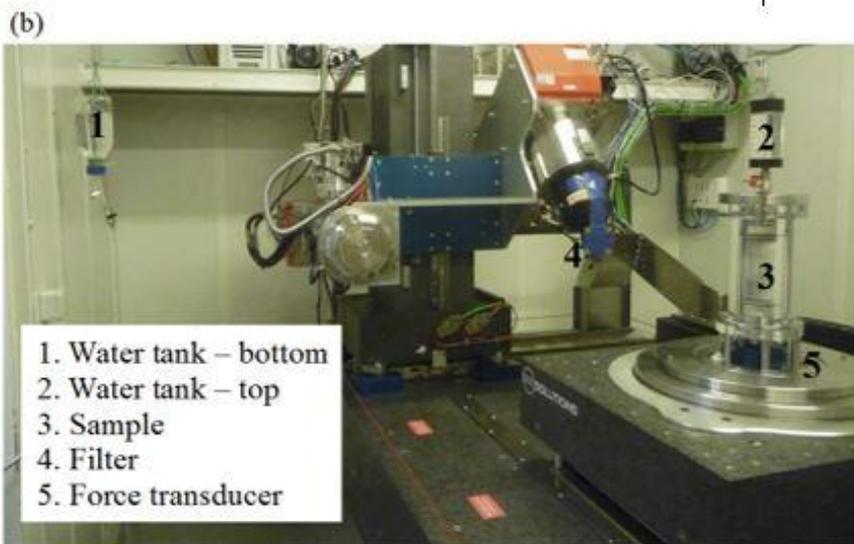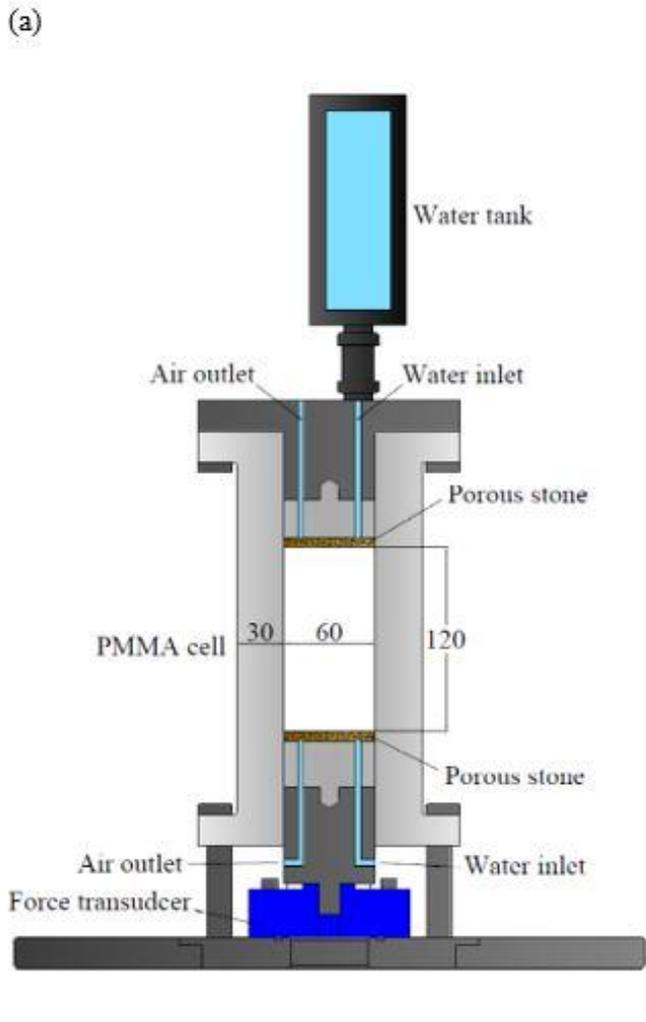
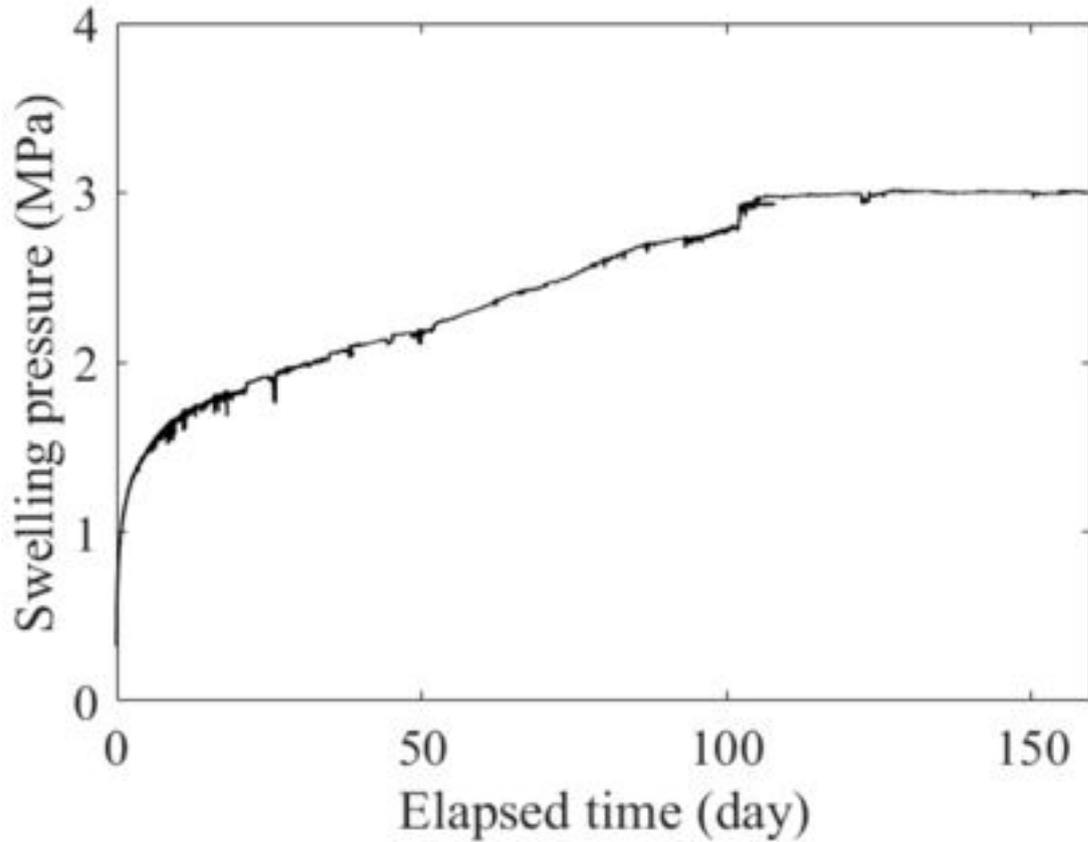Figure 2. Vertical sections of the sample at different times obtained by X-ray CT.

Figure 3. Enlargements of a horizontal section at 60 mm from the bottom obtained by X-ray
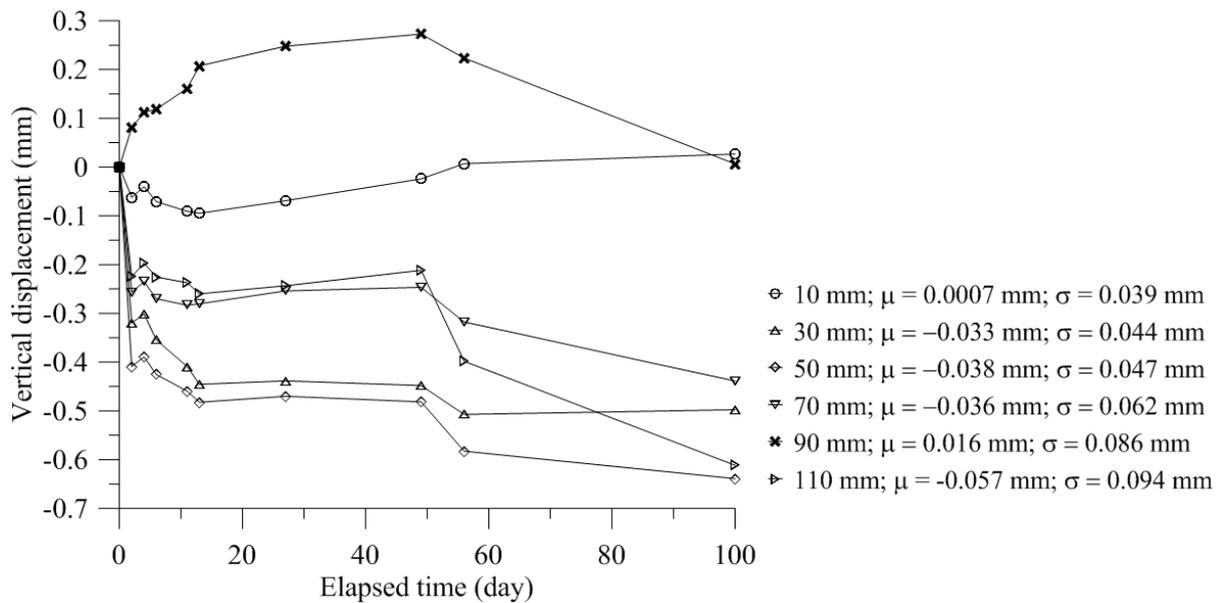CT.

401   Figure 4. Evolution of the axial swelling pressure of the mixture.

402

403

404   Figure 5. Vertical displacements obtained by Digital Volume Correlation (DVC) Technique
405   based on the PMMA spheres network while wetting.

406

407